Quantum Spin Liquid Emerging from Antiferromagnetic Order by Introducing Disorder

T. Furukawa,[1,*] K. Miyagawa,[1] T. Itou,[2] M. Ito,[3] H. Taniguchi,[3] M. Saito,[4] S. Iguchi,[4] T. Sasaki,[4] and K. Kanoda[1,†]
[1]Department of Applied Physics, University of Tokyo, Tokyo 113-8656, Japan
[2]Department of Applied Physics, Tokyo University of Science, Tokyo 125-8585, Japan
[3]Department of Physics, Saitama University, Saitama 338-8570, Japan
[4]Institute for Materials Research, Tohoku University, Sendai 980-8577, Japan
(Received 19 February 2015; revised manuscript received 2 June 2015; published 11 August 2015)

Quantum spin liquids, which are spin versions of quantum matter, have been sought after in systems with geometrical frustration. We show that disorder drives a classical magnet into a quantum spin liquid through conducting NMR experiments on an organic Mott insulator, κ-$(ET)_2Cu[N(CN)_2]Cl$. Antiferromagnetic ordering in the pristine crystal, when irradiated by x rays, disappears. Spin freezing, spin gap, and critical slowing down are not observed, but gapless spin excitations emerge, suggesting a novel role of disorder that brings forth a quantum spin liquid from a classical ordered state.

DOI: 10.1103/PhysRevLett.115.077001 PACS numbers: 74.70.Kn, 75.45.+j, 75.50.Lk, 76.60.-k

Quantum-disordered states in mutually interacting many-body systems are intriguing ground states that show no long-range order (LRO), even at absolute zero, owing to quantum fluctuations. The quest for such states is one of the most intensively studied issues in modern physics, because the states show a macroscopic quantum-entangled nature or emergent fractional excitations distinct from the constituent particles. Among quantum-disordered spin states are the quantum spin liquid (QSL) in Mott insulators with triangular, kagome, and hyperkagome lattices [1]. In these systems, geometrical frustration coming from the nonbipartite nature of lattices and/or charge fluctuations due to the vicinity of the Mott metal-insulator instability enhance the quantum fluctuations against antiferromagnetic LRO and are considered to hold a key for stabilizing the QSL states. In addition to the frustration, interplay between mutual interaction and quenched disorder, which is a fundamental issue argued not only in condensed matter physics [2–6] but also in the physics of cold atoms [7], can play a vital role in the quantum magnetism. In the present work, we demonstrate that disorder drives a classical LRO in a Mott insulator with a less frustrated lattice into a QSL. This result indicates that introducing disorder into strongly interacting electrons is a novel way to realize the quantum-disordered ground states.

A material used in the present study, κ-$(ET)_2Cu[N(CN)_2]Cl$ (κ-Cl), belongs to layered organic materials that are abbreviated as κ-$(ET)_2X$, where ET denotes bis(ethylenedithio)tetrathiafulvalene and X is an anion [Fig. 1(a)]. κ-$(ET)_2X$ are half-filled systems with anisotropic triangular lattices [8–10], where the anisotropy is defined by the ratio of transfer integrals, t'/t [Fig. 1(b)]. The substitution of X causes variations in the transfer integral (bandwidth) and the anisotropy of the triangular lattice (geometrical frustration). Various exotic ground states emerge: a Fermi liquid and an unconventional superconductor for $X = Cu[N(CN)_2]Br$ [11] with $t'/t \sim 0.4$–0.5 [12,13]; a Mott insulator with a commensurate antiferromagnetic LRO of $S = 1/2$ spins with an ordered moment of $0.45\mu_B$ (μ_B, Bohr magneton) for $X = Cu[N(CN)_2]Cl$ [14] with $t'/t \sim 0.4$–0.5 [12,13]; a QSL without magnetic LRO [15] for $X = Cu_2(CN)_3$ with $t'/t \sim 0.8$–1.0 [12,13]. These Mott insulating phases border on metallic and superconducting phases in a generic pressure-temperature phase diagram [16–18] [Fig. 1(c) for κ-Cl].

The effect of quenched disorder on the charge transport near the Mott transition has been explored by recent experiments using x-ray irradiation [19–21]. Optical studies sensitive to the chemical structure of the anion species indicate that the x-ray irradiation produces molecular defects in the anion layers, which are expected to cause randomness in electronic potential and/or transfer integrals in the ET layers [19]. For κ-$(ET)_2Cu[N(CN)_2]Br$, the low-temperature metallic resistivity increases with the irradiation time, followed by an Anderson-type insulating behavior [19,21]. For κ-Cl, the low-temperature insulating resistivity is decreased (for example, by 4 orders of magnitude at 10 K by an approximately 400-h irradiation [19]), and it is still insulating at low temperatures. The effect of disorder induced by x-ray irradiation in κ-$(ET)_2X$ increases with irradiation time and tends to become saturated after several hundred hours (approximately 500 h for κ-Cl [19]). What occurs in the spin degrees of freedom in this situation is an open question; more specifically, what is the fate of the antiferromagnetic LRO when the system suffers from quenched disorder? We pursue this issue by examining the spin state of the x-ray-irradiated κ-Cl, which shows antiferromagnetic LRO before being exposed to x rays, with ^1H NMR, which probes both the static and dynamic spin states through NMR spectra and the nuclear spin-lattice relaxation rate, respectively.

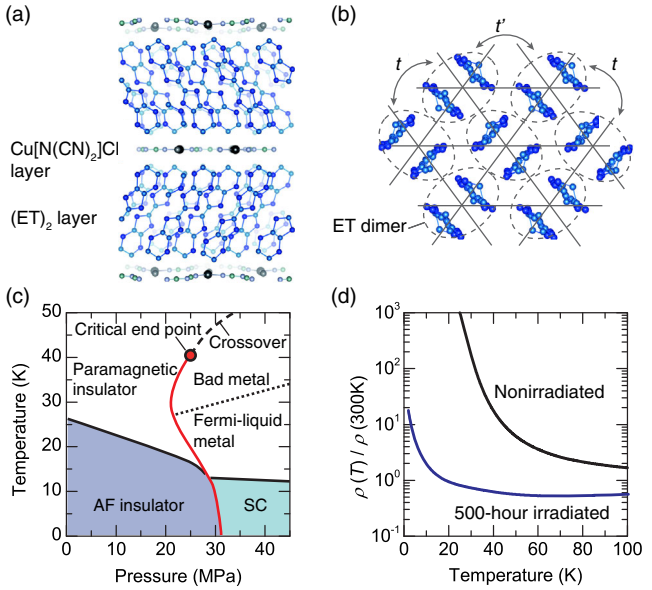

FIG. 1 (color online). Structure and transport properties of κ-Cl. (a) Layered structure of κ-Cl. (b) Structure of a conducting layer of κ-Cl. Transfer integrals between nearest-neighbor dimers (next-nearest-neighbor dimers) are shown as t (t'). (c) Pressure-temperature phase diagram of nonirradiated κ-Cl [16,17]. SC and AF denote superconductor and antiferromagnetic ordered state, respectively. (d) Temperature dependence of resistivity of the 500-h x-ray-irradiated (blue line) and nonirradiated (black line) κ-Cl crystals. The former crystal was used for the ^{1}H NMR study. The data for the latter were obtained in the previous study [19].

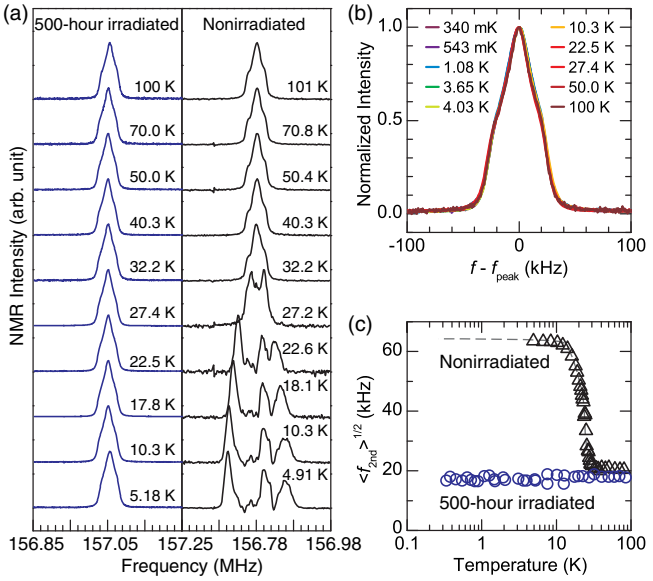

FIG. 2 (color online). Disappearance of antiferromagnetic order in the κ-Cl crystal after 500-h x-ray irradiation. (a) The temperature dependence of ^{1}H NMR spectra of the 500-h x-ray-irradiated and nonirradiated κ-Cl crystals. Some of the data for the latter are from our previous study [14]. (b) ^{1}H NMR spectra of the 500-h x-ray-irradiated κ-Cl crystal normalized to the maximum values at temperatures between 340 mK and 100 K. f_{peak} is the frequency at which the spectra have the maximum intensity. (c) The temperature dependence of the square root of the second moment of NMR spectra, $\langle f_{2\mathrm{nd}}\rangle^{1/2}$, for the 500-h x-ray-irradiated crystal (blue circles) and the nonirradiated crystal (black triangles); the latter is calculated from the spectra obtained in the previous study [14]. The dashed line guides the eye. The slight difference in the line shape and $\langle f_{2\mathrm{nd}}\rangle^{1/2}$ above 30 K between the two measurements is most likely due to a slight difference in the field geometry against the crystal axes, to which the line shape is sensitive.

A single crystal of κ-Cl was grown by using the electrochemical method. The sample was irradiated with white x rays at room temperature using a nonfiltered tungsten target at 40 kV and 20 mA [22]. The total irradiation time was 500 h, for which the irradiation is expected to induce a near-saturated amount of defects in κ-Cl [19]. We probed the spin state of the irradiated sample by ^{1}H NMR measurements under a magnetic field of 3.7 T applied perpendicular to the conducting plane at temperatures from 340 mK to 300 K [22]. We confirmed that the resistivity of the irradiated crystal is insulating at low temperatures, as shown in Fig. 1(d). The temperature dependence of resistivity is between the activation type and logarithmic type and is best approximated by the variable-range hopping model [22]. Furthermore, x-ray irradiation causes no appreciable Curie-like susceptibility [22].

Figures 2(a) and 2(b) show the temperature dependence of the NMR spectra for the nonirradiated and irradiated crystals. The line shape is the same in both cases at high temperatures, and the line width is reasonably explained by the nuclear dipole interaction between the protons in the ethylene groups of ET molecules. A clear difference appears below 30 K. In the nonirradiated crystal, the spectra exhibit splitting at the Néel temperature ($T_N \sim 27$ K [14]) owing to the generation of internal fields associated with the commensurate antiferromagnetic LRO. The temperature dependence of the splitting is characterized by the square root of the second moment of the NMR spectra in Fig. 2(c). The irradiated crystal, however, shows neither splitting nor broadening down to the lowest temperature measured, 340 mK, which is approximately 2 orders of magnitude lower than the Néel temperature of the nonirradiated crystal (Fig. 2). As shown in Fig. 2(b), the line shape is preserved over a wide temperature range, from 100 K down to 340 mK, providing unambiguous evidence for the absence of the spontaneous generation of the internal field. Thus, the results indicate that the antiferromagnetic LRO disappears after 500 h of x-ray irradiation, yet we rule out spin glass states, in which internal fields are generated.

The absence of the antiferromagnetic LRO and spin freezing is also shown by the nuclear spin-lattice relaxation rate T_1^{-1}, which is proportional to the local dynamic structure factor characterizing spin excitations. As observed in Fig. 3, T_1^{-1} of the x-ray-irradiated κ-Cl exhibits neither a

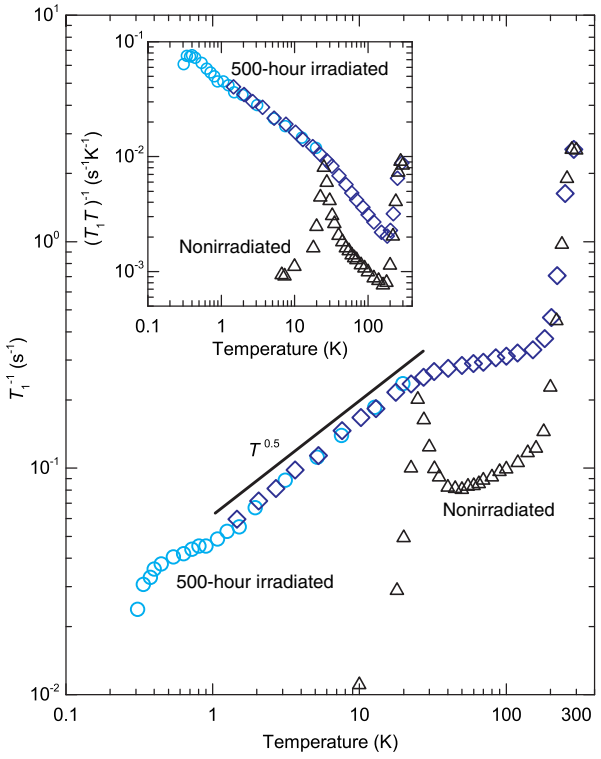

FIG. 3 (color online). Temperature dependence of the ^{1}H nuclear spin-lattice relaxation rate of κ-Cl. The main panel shows the ^{1}H nuclear spin-lattice relaxation rate T_1^{-1} of 500-h x-ray-irradiated and nonirradiated κ-Cl crystals. The inset shows $(T_1T)^{-1}$, where T is temperature. The light blue circles and dark blue diamonds correspond to the data acquired with the use of ^{3}He and ^{4}He cryostats [22], respectively. The black triangles are from the previous study of a nonirradiated κ-Cl crystal [14].

critical increase towards magnetic LRO nor a cusp structure due to spin freezing over the entire temperature range. This finding is in contrast to T_1^{-1} of the nonirradiated crystal, which shows a divergent peak at $T_N = 27$ K. A steep increase in T_1^{-1} above approximately 200 K is common to both samples and is due to the thermally activated vibration of ethylene groups located at the edges of the ET molecules, which outweighs the electronic contribution to T_1^{-1}. As the motional contribution to T_1^{-1} is diminished exponentially at lower temperatures, the observed relaxation, i.e., below 160 K, is electronic in origin. From 160 to 40 K, T_1^{-1} in the irradiated sample is nearly temperature independent, and the magnitude is enhanced by a factor of 3–4 by irradiation. At approximately 30 K, T_1^{-1} appears to cross over to a power law, $T_1^{-1} \propto T^{0.5}$, for temperatures down to approximately 1 K. This may suggest that the original Néel temperature $T_N = 27$ K may still be a characteristic temperature even in the irradiated crystal. This issue needs to be addressed in the future by studying the development of this anomaly in T_1^{-1} as a function of irradiation time. It is interesting that, below 1 K, T_1^{-1} shows a moderate humplike structure, reminiscent of the anomaly observed at approximately 6 K in the QSL state in κ-$(ET)_2Cu_2(CN)_3$ [25]. It is clear that the hump structure does not originate from a magnetic LRO or freezing, because there is no appreciable change in the NMR spectra.

The disappearance of magnetic LRO and the absence of a spin glass state in the irradiated crystal suggest a spin state that is markedly different from that of the nonirradiated system. The temperature dependence of the NMR spin-lattice relaxation rate gives insight into the nature of the spin state, because $(T_1T)^{-1}$ is proportional to the imaginary part of the $\boldsymbol{q}$-integrated dynamic susceptibility [to be exact, $\sum_{\boldsymbol{q}}\chi''(\boldsymbol{q},\omega_0)/\omega_0$, where $\boldsymbol{q}$ is the wave vector and ω_0 is the resonant frequency]. The temperature dependence of T_1^{-1} or $(T_1T)^{-1}$ provides evidence for gapless excitations that persist down to the lowest temperature and clearly rules out the possibility of nonmagnetic spin-gapped states, such as a valence bond crystal or a spin Peierls state. One possible gapless state conceivable in the present situation is an Anderson-type weakly localized metal. If such a metallic state were realized, $(T_1T)^{-1}$ would obey the Korringa law, $(T_1T)^{-1} \propto$ const [of the order of 10^{-3} s^{-1} K^{-1} for this type of organic compound, for example, κ-$(ET)_2Cu(NCS)_2$ [26]]. As shown in the inset in Fig. 3, $(T_1T)^{-1}$ monotonically increases at least down to 0.4 K and approaches a value of 10^{-1} s^{-1} K^{-1}, which appears inconsistent with the metallic state. Thus, we conclude that the present system is in a QSL state.

According to theoretical studies on the Hubbard or Heisenberg models, disorder-induced gapless states without LRO can emerge on a square lattice ($t'/t = 0$) [27,28]. Recently, it has been reported that the bond-random $S = 1/2$ Heisenberg model on a triangular lattice with a spatially random exchange coupling exhibits a random singlet state with gapless QSL features [29]. Noticeably, the 120° Néel order transforms into the random singlet without the emergence of a spin glass state as bond randomness is increased. Considering that a singlet is a purely quantum state, the theoretical result suggests that the randomness makes the quantum nature of spins emerge. As mentioned above, the present system is near the Mott metal-insulator transition [16,17]; thus, the localized wave function, if subject to external perturbations, tends to be extended. We speculate that the random singlets in the strong correlation limit become mutually entangled and long ranged to yield a gapless nature near the metal-insulator transition, such as a "spin liquid Bose glass" or a "diffusive spinon metal," as proposed in recent theoretical studies [3,4].

Next, we discuss a possible macroscopic inhomogeneity induced by the x-ray irradiation. In general, the relaxation curve of nuclear magnetization, $\log[1 - M(t)/M_0]$ vs t [where t is the time of recovery, $M(t)$ is the magnetization of the nuclear spin, and M_0 is a saturated value of $M(t)$], falls in a straight line characterized by a single spin-lattice

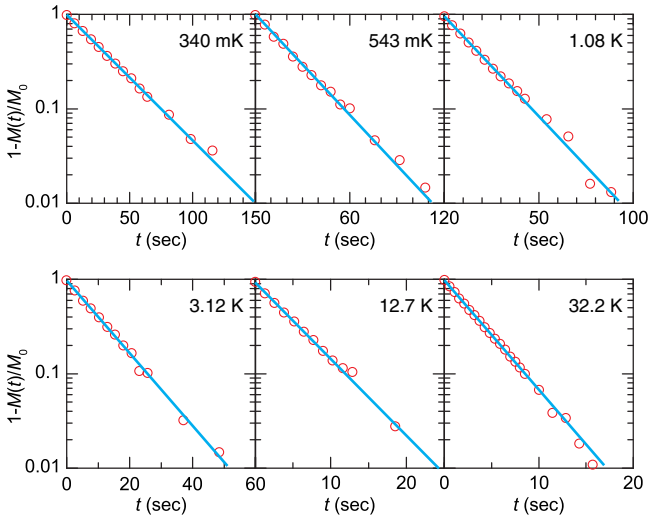

FIG. 4 (color online). ^{1}H NMR relaxation curves. The recovery of nuclear magnetization $M(t)$ is plotted in the form of $\log[1-M(t)/M_0]$ vs t for several temperatures. All of the data, including those not shown here, are well fitted by straight lines: $1-M(t)/M_0 \propto \exp(-t/T_1)$ with T_1 nuclear spin-lattice relaxation time.

relaxation time T_1 when the system is homogeneous. By contrast, in the inhomogeneous case, the relaxation curve is bent because of the distribution of the spin-lattice relaxation rate. As shown in Fig. 4, the relaxation curves in the present experiments are all straight lines for every temperature down to 340 mK. Although it is likely that the so-called T_2 process between ^{1}H nuclear dipoles averages the inhomogeneity in T_1^{-1} on the order of the length scale of the lattice constant, a macroscopic inhomogeneity is ruled out.

Finally, we compare the present results with the behaviors of the QSLs in nearly isotropic triangular lattices, κ-$(ET)_2Cu_2(CN)_3$ [15,25] and $EtMe_3Sb[Pd(dmit)_2]_2$ [30]. These two compounds host gapless or marginally gapless QSLs [31,32]. For probing the spin states, ^{1}H and ^{13}C T_1^{-1} are available for κ-$(ET)_2Cu_2(CN)_3$, whereas only ^{13}C T_1^{-1} is available for $EtMe_3Sb[Pd(dmit)_2]_2$, where ^{1}H T_1^{-1} is dominated by the methyl rotational motion from 10 to 100 K. Regardless of materials and observed nucleus, the temperature dependence of T_1^{-1} of the original QSLs shows three characteristic behaviors: namely, $T_1^{-1} \propto T^{0.5}$ at high temperatures [$T > 10$ K for κ-$(ET)_2Cu_2(CN)_3$, $T > 5$ K for $EtMe_3Sb[Pd(dmit)_2]_2$], a plateau or a moderate increase in T_1^{-1} on cooling at intermediate temperatures of 1–5 K, and gapless behaviors, $T_1^{-1} \propto T^{\alpha}$ [$\alpha = 1$–2 (^{1}H), 1.5 (^{13}C) for κ-$(ET)_2Cu_2(CN)_3$, $\alpha = 2$ for $EtMe_3Sb[Pd(dmit)_2]_2$] at low temperatures below 0.5 K accompanied by inhomogeneous nature in the spectra and the NMR relaxations. The x-ray-irradiated κ-Cl even shows the common $T_1^{-1} \propto T^{0.5}$ behavior down to 1 K in a different temperature range from the original QSL cases. Although T_1^{-1} deviates from the $T^{0.5}$ dependence below 1 K, it is much more moderate than in the two QSLs. The change of the behavior to different power laws at lower temperatures in the two original QSLs is accompanied by inhomogeneity, although in different ways between the two. This inhomogeneity is missing in the present case, making a crucial difference from the original QSL cases. In general, disorder induces inhomogeneity in an electronic state; thus, the original QSLs exhibiting inhomogeneity can be a disorder-driven QSL suggested in Ref. [29]. However, this viewpoint contradicts the fact that κ-$(ET)_2Cu_2(CN)_3$ under pressure is a good metal with a residual resistivity ratio of several hundreds and exhibits superconductivity [18]; that is, the extent of disorder in κ-$(ET)_2Cu_2(CN)_3$, if any, is less by far than required for the disorder-driven QSL in Ref. [29] (distribution in exchange interaction by several tens percent). Yet, the fact that the present system with more disorder is more homogeneous is inconsistent with this picture. Alternatively, the inhomogeneity in the original QSLs is associated with anomalies in T_1^{-1}, which can be manifestations of possible instabilities in QSLs as suggested theoretically, e.g., the instabilities of spinon Fermi surfaces [33,34] reminiscent of the pairing instabilities in metals. It may be the case that such instabilities are suppressed by disorder. As another origin of the difference between the original QSL and the present one, different degrees of frustration are conceivable. QSLs emerge from degenerate or competing phases, which should be different for different values of t'/t. For the present QSL ($t'/t \sim 0.5$), a competing phase is a collinear Néel state, while for κ-$(ET)_2Cu_2(CN)_3$ and $EtMe_3Sb[Pd(dmit)_2]_2$ with $t'/t \sim 1$, a likely competing phase is a 120° Néel state. Thus, the nature of the QSLs can differ for different values of t'/t, and the possible emergence of instabilities associated with the observed inhomogeneity is expected to depend on t'/t.

We emphasize that the disappearance of antiferromagnetic order in response to x-ray irradiation is accompanied by a disorder effect on the charge degrees of freedom, as shown by the resistivity behavior after x-ray irradiation. The emerging spin state, however, exhibits no spin freezing, no spin gap, and no critical slowing down toward ordering. Instead, this state shows some properties common to the original QSLs, in which deconfined mobile spinons would be responsible for low-energy excitations [31,32]. This implies that mobile spinons would appear in the present QSL in the irradiated κ-Cl as well. Considering the fact that the irradiated κ-Cl is a disordered Mott insulator close to the metal-insulator transition, the present QSL might be consistent with a theoretical suggestion that, near the Mott-Anderson transition, a QSL with mobile spinons is hosted by a spinon-deconfined chargon-glass insulator [3]. The present results provide the perspective that spinon-deconfined states are ubiquitous in situations where interactions and randomness induced by disorder both play vital roles in electron localization, even if geometrical frustration is not prominent.

This work was supported in part by JSPS KAKENHI under Grants No. 20110002, No. 25220709, No. 24654101, and No. 25287080, the U.S. National Science Foundation under Grant No. PHYS-1066293, and the hospitality of the Aspen Center for Physics.

*Present address: Department of Applied Physics, Tokyo University of Science, Tokyo 125-8585, Japan.
Corresponding author.
tetsuya.furukawa@rs.tus.ac.jp
†Corresponding author.
kanoda@ap.t.u-tokyo.ac.jp

[1] L. Balents, Nature (London) **464**, 199 (2010).
[2] D. Belitz and T. R. Kirkpatrick, Rev. Mod. Phys. **66**, 261 (1994).
[3] K.-S. Kim, Phys. Rev. B **73**, 235115 (2006).
[4] A. C. Potter, M. Barkeshli, J. McGreevy, and T. Senthil, Phys. Rev. Lett. **109**, 077205 (2012).
[5] K. Byczuk, W. Hofstetter, and D. Vollhardt, Phys. Rev. Lett. **94**, 056404 (2005).
[6] E. C. Andrade, E. Miranda, and V. Dobrosavljević, Phys. Rev. Lett. **102**, 206403 (2009).
[7] L. Sanchez-Palencia and M. Lewenstein, Nat. Phys. **6**, 87 (2010).
[8] H. Kino and H. Fukuyama, J. Phys. Soc. Jpn. **65**, 2158 (1996).
[9] K. Kanoda and R. Kato, Annu. Rev. Condens. Matter Phys. **2**, 167 (2011).
[10] B. J. Powell and R. H. McKenzie, Rep. Prog. Phys. **74**, 056501 (2011).
[11] A. M. Kini, U. Geiser, H. H. Wang, K. D. Carlson, J. M. Williams, W. K. Kwok, K. G. Vandervoort, J. E. Thompson, and D. L. Stupka, Inorg. Chem. **29**, 2555 (1990).
[12] H. C. Kandpal, I. Opahle, Y.-Z. Zhang, H. O. Jeschke, and R. Valentí, Phys. Rev. Lett. **103**, 067004 (2009).
[13] T. Koretsune and C. Hotta, Phys. Rev. B **89**, 045102 (2014).
[14] K. Miyagawa, A. Kawamoto, Y. Nakazawa, and K. Kanoda, Phys. Rev. Lett. **75**, 1174 (1995).
[15] Y. Shimizu, K. Miyagawa, K. Kanoda, M. Maesato, and G. Saito, Phys. Rev. Lett. **91**, 107001 (2003).
[16] S. Lefebvre, P. Wzietek, S. Brown, C. Bourbonnais, D. Jérome, C. Mézière, M. Fourmigué, and P. Batail, Phys. Rev. Lett. **85**, 5420 (2000).
[17] F. Kagawa, K. Miyagawa, and K. Kanoda, Nature (London) **436**, 534 (2005).
[18] Y. Kurosaki, Y. Shimizu, K. Miyagawa, K. Kanoda, and G. Saito, Phys. Rev. Lett. **95**, 177001 (2005).
[19] T. Sasaki, Crystals **2**, 374 (2012).
[20] J. G. Analytis, A. Ardavan, S. J. Blundell, R. L. Owen, E. F. Garman, C. Jeynes, and B. J. Powell, Phys. Rev. Lett. **96**, 177002 (2006).
[21] K. Sano, T. Sasaki, N. Yoneyama, and N. Kobayashi, Phys. Rev. Lett. **104**, 217003 (2010).
[22] See Supplemental Material at http://link.aps.org/supplemental/10.1103/PhysRevLett.115.077001 for experimental details and supporting results, which includes Refs. [23,24].
[23] B. L. Henke, E. M. Gullikson, and J. C. Davis, At. Data Nucl. Data Tables **54**, 181 (1993).
[24] A. L. Efros and B. I. Shklovskii, J. Phys. C **8**, L49 (1975).
[25] Y. Shimizu, K. Miyagawa, K. Kanoda, M. Maesato, and G. Saito, Phys. Rev. B **73**, 140407 (2006).
[26] T. Takahashi, T. Tokiwa, K. Kanoda, H. Urayama, H. Yamochi, and G. Saito, Synth. Met. **27**, A319 (1988).
[27] A. W. Sandvik and M. Vekić, Phys. Rev. Lett. **74**, 1226 (1995).
[28] M. Ulmke and R. T. Scalettar, Phys. Rev. B **55**, 4149 (1997).
[29] K. Watanabe, H. Kawamura, H. Nakano, and T. Sakai, J. Phys. Soc. Jpn. **83**, 034714 (2014).
[30] T. Itou, A. Oyamada, S. Maegawa, and R. Kato, Nat. Phys. **6**, 673 (2010).
[31] S. Yamashita, Y. Nakazawa, M. Oguni, Y. Oshima, H. Nojiri, Y. Shimizu, K. Miyagawa, and K. Kanoda, Nat. Phys. **4**, 459 (2008).
[32] M. Yamashita, N. Nakata, Y. Senshu, M. Nagata, H. M. Yamamoto, R. Kato, T. Shibauchi, and Y. Matsuda, Science **328**, 1246 (2010).
[33] S.-S. Lee, P. A. Lee, and T. Senthil, Phys. Rev. Lett. **98**, 067006 (2007).
[34] V. Galitski and Y. B. Kim, Phys. Rev. Lett. **99**, 266403 (2007).